16th European Signal Processing Conference (EUSIPCO 2008), Lausanne, Switzerland, August 25-29, 2008, copyright by EURASIP

ROBUST MULTIPLICATIVE WATERMARKING TECHNIQUE WITH MAXIMUM LIKELIHOOD DETECTOR

S.M.E. Sahraeian, M.A. Akhaee, B. Sankur[*]*, and F. Marvasti*

Advanced Communications Research Institute (ACRI)
Department of Electrical Engineering, Sharif University of Technology
[*] Department of Electrical-Electronic Engineering, Bogazici University
Azadi Ave., Tehran, Iran
phone: +(98) 21 66165910, fax: +(98) 21 66036002
email: msahraeian@ee.sharif.edu, akhaee@ee.sharif.edu, bulent.sankur@boun.edu.tr, marvasti@sharif.edu

ABSTRACT

In this paper, a new multiplicative semi-blind image-adaptive watermarking system has been presented, which exploits human visual model for adapting the watermark data to local properties of the host image. To have a better robustness, the proposed algorithm is implemented on the low-frequency coefficients of the wavelet transform. Moreover, regarding invisibility of the algorithm, the strength factor which controls the watermark power is optimally selected. To extract the watermark data, the Maximum Likelihood (ML) estimator is used. Experimental results confirm the imperceptibility of the proposed method and its high robustness against various attacks such as JPEG compression, noise addition, and filtering compared to similar methods reported so far.

1. INTRODUCTION

Digital watermarking is a process in which some information is embedded within a digital media so that the inserted data becomes part of the media. This technique serves a number of purposes such as broadcast monitoring, data authentication, data indexing and so fourth. A digital watermarking system must successfully satisfy trade-offs between conflicting requirements of perceptual transparency, data capacity and robustness against attacks.

Multiplicative watermarking is one of the most popular approaches for copy right protection where the watermark is served as a verification code. Since this technique is image content dependent, higher robustness is achieved than other techniques such as additive watermarking methods.

The correlation detector is used for multiplicative watermarking in [1]; however, this type of detection is not suitable when the watermarking is performed in the transform domain. Hence, for the Barni's multiplicative watermarking method in the transform domain [2], several optimum and locally optimum decoders have been proposed so far [3],[4]. In [3], a robust optimum detector for the multiplicative rule $y_i = x_i(1+\alpha_i w_i)$ in the DCT, DWT and DFT domains is proposed.

In this paper, in order to achieve higher robustness against various attacks, a multiplicative semi-blind watermarking approach in the wavelet transform domain is used. In our implementation, the host image is segmented into small blocks and high entropy blocks are chosen. In each block, low-frequency wavelet coefficients are multiplied or divided by the strength factor (a constant value) depending on the value of the watermark bits. The strength factor is optimized both to minimize the impact on the quality of the image [5], and to obtain the best detection performance. For data extraction, similar to [2],[6], the ML detector is used. We model the low frequency wavelet coefficients of blocked images with Gaussian distribution. Under this assumption, the optimum threshold and error probability of the proposed multiplicative watermarking method are analytically calculated. Besides, analytical formulations of performance analysis for this decision-theoretic problem under Gaussian signal and Gaussian noise conditions are presented.

2. PROPOSED METHOD

2.1 Watermark embedding

Imperceptibility of watermarking can be improved by exploiting the characteristics of the HVS. According to the entropy masking of Watson's visual model [7], we utilize high entropy blocks of an image to insert our image-dependent watermarking scheme. That is, we segment the host image into non-overlapping blocks and choose the N blocks with the highest entropy for the watermarking purpose. Typical block sizes are 16x16.

We embed a single bit of '0' or '1' to each selected high entropy block by manipulating the wavelet coefficients in the last approximation scale based on the following strategy. Let X_i be the i^{th} block of the image. If $i = \arg(Entropy(X_i) > Threshold)$, then we embed the bit in this block using:

$$W_i' = \begin{cases} W_i \cdot \alpha & \text{For embedding '1'} \\ W_i \cdot \frac{1}{\alpha} & \text{For embedding '0'} \end{cases} \quad (1)$$

where W_i is the wavelet coefficients in the last approximation scale of the image block X_i, and α is varied in an appropriate range and is called the strength factor.

Any visible effect, such as blocking, due to the manipulation of wavelet coefficients is controlled using a parameter optimization method as in Section 2.4. The watermarked image is obtained by inverse DWT of the watermarked coefficients W_i' to get the watermarked block image X_i'.

2.2 Watermark detection

Our detector is equipped with the information of block positions and their mean and variance. Hence we can optimize the decision process for each block. To extract the hidden bit in each block, we implement an optimum detector as follows.

We assume as in [8] that these approximation coefficients have Gaussian distribution, with known mean and variance due to side information channel.

We consider a generic block chosen for watermarking and let w_i represent the wavelet coefficients of the approximation band used for watermark embedding with mean μ and variance σ^2. After data embedding, depending on the message bit (0/1), these coefficients are multiplied or divided by the strength factor α.

At the receiver, after noise or other attacks, we receive the coefficients y_i which are the w_i coefficients contaminated by zero mean AWGN. In other words, we model the effect of attacks simply as AWGN. Since both wavelet approximation band coefficients and noise are iid and Gaussian distributed, the distribution of y for '1' or '0' embedding can be written as:

$$y_{i|1} = \alpha \cdot w_i + n_i \Longrightarrow y_{i|1} \sim N(\alpha\mu, \sigma^2_{y_{|1}}) \tag{2}$$

$$y_{i|0} = \alpha^{-1} \cdot w_i + n_i \Longrightarrow y_{i|0} \sim N(\alpha^{-1}\mu, \sigma^2_{y_{|0}}) \tag{3}$$

where $\sigma^2_{y_{|1}} = \alpha^2\sigma^2 + \sigma^2_n$ and $\sigma^2_{y_{|0}} = \alpha^{-2}\sigma^2 + \sigma^2_n$. Furthermore, σ^2_n is the variance of the noise in the related subband, which can be estimated as follows. If we show the noise standard deviation in the image by $\hat{\sigma}$, it can be estimated from the HH_1 wavelet subband, the first detail subband, by the robust median estimator, suggested in [9].

By estimating $\hat{\sigma}$, we can find the noise standard deviation in the last lowpass scale σ_n as $\sigma_n = \|L\|\hat{\sigma}$, where L is the unit sample response of the filter that generates the approximation band. Moreover, $\|.\|$ is the norm operator: $\|L\| = \sqrt{\sum_l \sum_k L^2(l,k)}$.

In our model, wavelet coefficients are assumed to be i.i.d.. Since the wavelet coefficients are decimated in each level of decomposition, this assumption is nearly satisfactory. Therefore, the distribution of these coefficients in a specific block with N coefficients $y_1, y_2, ..., y_N$ for '1' or '0' embedding is:

$$P(y_1, y_2, ..., y_N|1) = \prod_{i=1}^{N} \frac{1}{\sqrt{2\pi\sigma^2_{y_{|1}}}} \cdot e^{-\frac{(y_i-\alpha\mu)^2}{2\cdot\sigma^2_{y_{|1}}}} \tag{4}$$

$$P(y_1, y_2, ..., y_N|0) = \prod_{i=1}^{N} \frac{1}{\sqrt{2\pi\sigma^2_{y_{|0}}}} \cdot e^{-\frac{(y_i-\alpha^{-1}\mu)^2}{2\cdot\sigma^2_{y_{|0}}}} \tag{5}$$

In order to have Maximum Likelihood (ML) decision we must have:

$$P(y_1, y_2, ..., y_N|1) \gtrless_0^1 P(y_1, y_2, ..., y_N|0) \tag{6}$$

Thus, by substituting (4) and (5) in (6), and after some simplifications, we have:

$$\begin{aligned}(\frac{1}{\sigma^2_{y_{|0}}} - \frac{1}{\sigma^2_{y_{|1}}})\sum_{i=1}^{N} y_i^2 - 2\mu(\frac{\alpha^{-1}}{\sigma^2_{y_{|0}}} - \frac{\alpha}{\sigma^2_{y_{|1}}})\sum_{i=1}^{N} y_i \\ \gtrless_0^1 2Nln(\frac{\sigma_{y_{|1}}}{\sigma_{y_{|0}}}) - N\mu^2(\frac{\alpha^{-2}}{\sigma^2_{y_{|0}}} - \frac{\alpha^2}{\sigma^2_{y_{|1}}})\end{aligned} \tag{7}$$

Through (2),(3) and (7), the best decision depends obviously on the estimate of the noise variance σ^2_n. If we can obtain an appropriate estimation of the noise, the decision is made according to (7). Consider the detector at the limiting values for high SNR, that is $\sigma_n \to 0$, one has:

$$(\alpha^4 - 1)\sum_{i=1}^{N} y_i^2 - 2\alpha(\alpha^2 - 1)\sum_{i=1}^{N} y_i \gtrless_0^1 4N\alpha^2\sigma^2 ln(\alpha) \tag{8}$$

2.3 Error Probability

The error probability of the proposed technique in detecting the watermarked data stream in presence of noise can be shown to be as follows:

$$\begin{aligned} P_e &= \frac{1}{2}P_{e|1} + \frac{1}{2}P_{e|0} \\ &= \frac{1}{2}\{[\frac{c_1 a_1}{a_2}\int_0^{\infty}\gamma(\tfrac{N}{2}, \tfrac{x}{2})e^{-\frac{(\frac{T'-a_1 x}{a_2} - N\alpha\mu)^2}{2N\sigma^2_{y_{|1}}}}dx] \\ &+ [1 - \frac{c_2 b_1}{b_2}\int_0^{\infty}\gamma(\tfrac{N}{2}, \tfrac{x}{2})e^{-\frac{(\frac{T''-b_1 x}{b_2} - N\alpha^{-1}\mu)^2}{2N\sigma^2_{y_{|0}}}}dx]\} \end{aligned} \tag{9}$$

where $c_1 = \frac{1}{\sqrt{2\pi N\sigma^2_{y_{|1}}}}$, $c_2 = \frac{1}{\sqrt{2\pi N\sigma^2_{y_{|0}}}}$ and

$$a_1 = \zeta\sigma^2_{y_{|1}}, \quad a_2 = 2\alpha\mu\zeta + \xi, \quad T' = T + \zeta N\alpha^2\mu^2$$

$$b_1 = \zeta\sigma^2_{y_{|0}}, \quad b_2 = 2\alpha^{-1}\mu\zeta + \xi, \quad T'' = T + \zeta N\alpha^{-2}\mu^2$$

Moreover,

$$\zeta = (\frac{1}{\sigma^2_{y_{|0}}} - \frac{1}{\sigma^2_{y_{|1}}}), \qquad \xi = 2\mu(\frac{\alpha}{\sigma^2_{y_{|1}}} - \frac{\alpha^{-1}}{\sigma^2_{y_{|0}}}),$$

$$T = 2Nln(\frac{\sigma_{y_{|1}}}{\sigma_{y_{|0}}}) - N\mu^2(\frac{\alpha^{-2}}{\sigma^2_{y_{|0}}} - \frac{\alpha^2}{\sigma^2_{y_{|1}}})$$

The function $\gamma(a,x) = \frac{1}{\Gamma(a)}\int_0^x e^{-t}t^{a-1}dt$ is called the lower incomplete gamma function. Due to the lack of space the detailed proof is omitted. We utilize the above error probability function in optimizing the parameter α as discussed in the following section.

2.4 Parameter Optimization

The parameter α has a critical effect on the performance of the watermarking scheme. Its value can affect two factors in the watermarked image: visibility and robustness. Since there is a trade-off between visibility and robustness, we utilize a multi-objective optimization technique to select an appropriate value for α which ensures imperceptibility with acceptable robustness.

To show the effect of the α parameter on the distortion occurring in the image, we use the image quality index Q suggested in [5]. In this quality assessment method, any image distortion is modeled as a combination of three factors considering the properties of the HVS: loss of correlation, luminance distortion, and contrast distortion. This image quality index outperforms traditional quality assessment methods such as MSE due to its conformity to HVS and subjective tests.

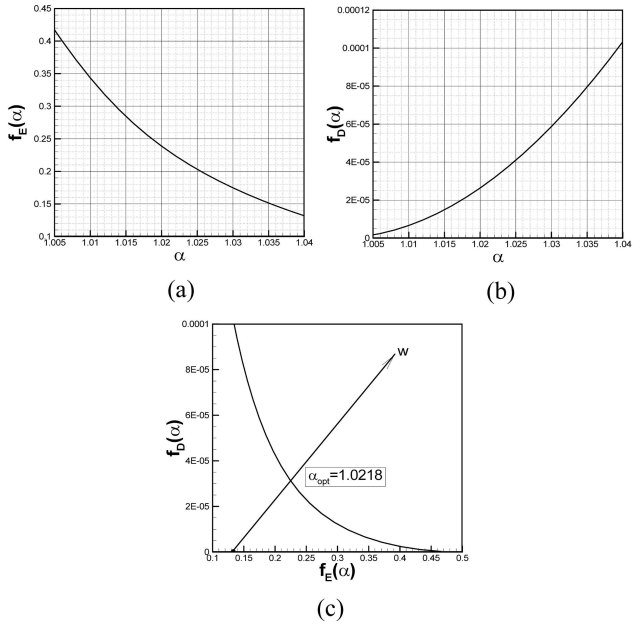

Figure 1: An example of implementing the goal attainment optimization method to find the optimum α parameter.

If we denote the original and the watermarked images with x and y, respectively ,the quality index Q is defined as:

$$Q = \frac{(\hat{x}\hat{y}+C_1)(2\sigma_{xy}+C_2)}{[(\hat{x})^2+(\hat{y})^2+C_1](\sigma_x^2+\sigma_y^2+C_2)} \qquad (10)$$

where $\hat{x}$, $\hat{y}$, σ_x^2, and σ_y^2 are the mean values and variances of x and y, respectively. Moreover, parameters C_1 and C_2 are defined as $C_1 = (K_1L)^2$, $C_2 = (K_2L)^2$, where L is the dynamic range of the pixel values (255 for 8-bit grayscale images), and $K1, K2 \ll 1$ are small constants (we choose $K_1 = 0.01$ and $K_2 = 0.03$ throughout this paper). The dynamic range of Q is $[-1,1]$. The best value 1 is achieved if and only if $y_i = x_i$ for all $i = 1,2,...,N$. Since image signals are generally non-stationary and image quality is often spatially variant, we measure statistical features locally and then combine them together using geometric averaging.

Thus, we have two objective functions : $f_D(\alpha)$, which reveals the effect of α on the distortion and is calculated as $f_D(\alpha) = 1 - Q(\alpha)$, and $f_E(\alpha)$, which exhibits the robustness and is calculated as the error probability function in (9). The first objective function is monotonically increasing with α, while the second one is monotonically decreasing. Our goal is to find an optimum value of alpha which minimizes both these objective functions. However, given the very different nature of the two objective functions, we cannot sum them. Thus, we treat it as a multi-objective optimization problem.

To solve this problem, we use the goal attainment method of Gembicki [10]. In this method, to optimize a set of m objective functions $F(x) = [F_1(x), F_2(x), ..., F_m(x)]$ which have some trade-offs, a set of design goals, $F^* = [F_1^*, F_2^*, ..., F_m^*]$ and a set of weights, $w = [w_1, w_2, ..., w_m]$ are considered. Then, the goal attainment problem can be formulated as:

$$\min_{\lambda \in \Re} \lambda \qquad \text{subject to} \qquad F_i(x) - w_i\lambda \le F_i^* \quad , \quad i = 1,2,..,m, \qquad x \in \Omega \qquad (11)$$

Table 1: Comparing the effect of block size and code length on the robustness of the proposed methods (results are in BER(%)).

Block Size	Code Length (bits)	*Boat* JPEG (Q=10%)	*Boat* Noise (σ_n=20)	*Boat* Med. (3×3)	*Peppers* JPEG (Q=10%)	*Peppers* Noise (σ_n=20)	*Peppers* Med. (3×3)
8	128	16.09	10.90	13.59	19.22	10.51	3.28
8	256	16.35	9.04	11.19	17.05	12.60	2.87
8	512	20.58	13.79	11.13	22.72	15.13	3.03
8	1024	23.13	16.86	10.22	24.37	18.09	3.11
8	2048	24.39	17.22	7.43	26.75	19.50	2.78
16	128	**1.45**	**1.64**	**3.44**	3.09	**1.45**	**0.39**
16	256	5.35	3.98	**3.44**	6.78	5.33	0.92
16	512	6.74	4.45	3.89	8.82	7.16	0.80
32	128	2.93	1.91	5.00	**2.27**	2.07	0.47
32	256	15.02	10.43	5.74	22.11	17.60	2.93

where, Ω is the feasible region in the parameter space x and λ is an auxiliary variable unrestricted in sign. The weight vector, w, enables the designer to select trade-offs between the objectives. That is, if we can tolerate an objective to be under-attained, a smaller weight is assigned to it; conversely if we require objective to be over-attained, then a larger weight must be assigned to it.

As an example, Fig. 1(a),(b) show the two objective functions $f_E(\alpha)$ and $f_D(\alpha)$ versus different values of α for *Barbara* test image. Fig. 1(c) illustrates the goal attainment optimization method for this test case, where $f_E(\alpha)$ has been plotted versus $f_D(\alpha)$, with α parametrically varying. As we see the optimum value of α is obtained as 1.0218. The same strategy is implemented for each image to find the optimum α parameter.

3. EXPERIMENTAL RESULTS

We have performed several experiments to test the proposed algorithms and evaluate its performance against various kinds of attacks. Throughout our experiments, we use the Daubechies length-8 Symslet filters with three levels of decomposition to compute the 2-D DWT. The watermark data is embedded in the third level approximation coefficients of each block. The results are obtained by averaging over 20 runs with 20 different pseudorandom binary sequences as the watermarking signal.

For this study, we use various natural images of size 512×512. These images consist of *Barbara*, *Boat*, *Baboon*, *Plane*, *Peppers*, and *Goldhill*. The watermarked test images using the proposed method are shown in Fig. 2. As we can see, the watermark invisibility is satisfied. The mean Peak-Signal-to-Noise-Ratio (PSNR) of the watermarked images are 48.15dB, 47.14dB, 46.65dB, 45.61db, and 47.08db, 47.26 respectively.

In the first experiment, we investigate the effect of the block size and the message size on the proposed method. Note that we take the message size the same as the number of blocks, so that we guarantee to have always enough blocks for bits. BER results after different attacks for different images are given in Table 1. We have experimented with various block sizes and code lengths, and we chose the case of 16×16 block sizes with 128 bit code words as this combination yielded the lowest bit error rate. Nevertheless, other cases can be used depending on the requirements. The watermarked images shown in Fig. 2 are achieved with these selections. For other simulations we use this block size and code length.

Figure 2: Watermarked test images : *Barbara*, *Boat*, *Baboon*, *Plane*, *Peppers*, and *Goldhill*

In the second set of experiments, we test the performance using the well-known StirMark attack set using the parameter settings obtained in the first set of experiments. Table 2 show the BER results for median filtering, and Gaussian low-pass filtering attack with different test images. It can be seen that the proposed scheme is highly robust against various attacks.

Moreover, JPEG compression attack and AWGN attack are investigated in Fig. 3 and 4. These figures verify that the scheme exhibits strong resistance against JPEG attack with a quality factor of up to 10% and against intense noise attacks even with $\sigma_n = 30$.

In the next experiment we evaluate P_e the probability of error calculated in (9). To this aim, we calculate BER for a Gaussian random variable watermarked by the proposed method. The BER result accompanied by BER results of our ML watermark detector for this signal is shown in Fig. 5. We can see that the theoretical and experimental results match perfectly. Besides, the average BER for 100 different test images are shown. We can see that the model used for image blocks well agree with the theoretical result.

To compare our watermarking algorithm with other watermarking schemes, we perform the simulation to embed watermark with the same bit rate and PSNR as the bit rate and PSNR used in other techniques. The results are shown in Tables 3-6.

In Tables 3-5 we compared our watermarking scheme with the MWT-EMD method [11] for the code length of 64 bits and PSNR (42 dB) for the watermarked image as used in [11] with the *Baboon*, *Peppers*, and *Goldhill* images against JPEG compression, AWGN and median filtering attacks. The tables confirm that our watermarking method has better performance than the MWT-EMD method [11].

Table 2: BER(%) Results of extracted watermark under median and Gaussian filtering attacks

Image	Median Filtering		Gaussian Filtering		
	3×3	5×5	3×3	5×5	7×7
Barbara	3.83	16.02	1.17	4.10	4.14
Boat	3.79	15.55	0.00	0.00	0.00
Baboon	4.53	16.56	1.13	4.22	4.30
Plane	5.20	18.20	0.47	1.05	1.33
Peppers	0.23	3.05	0.00	0.90	0.90
Goldhill	0.39	2.81	0.00	0.82	0.82

Finally, we compare our method with Tsai's Wavelet Tree Group Modulation (WTGM) method [12] in Table 6. In this table, we embed 512 data bits in *Peppers* and *Goldhill* images with respective PSNR (39.8 dB) and (38.7 dB) for the watermarked image as in [12]. The superiority of our method over [12] which is a non-blind technique is obvious.

4. CONCLUSION

In this paper, we have presented a new semi-blind multiplicative image watermarking technique in the wavelet domain. The watermark data is embedded in the lowpass wavelet coefficients of each selected block using a new multiplicative method. An optimum ML detector is used to detect the embedded watermark code at the receiver end. Moreover, we implemented a multi-objective optimization approach to find the best possible strength factor α to increase the robustness regarding to the transparency. Conducting several experiments, the robustness of the proposed method against several attacks and its higher performance in comparison with various watermarking techniques is verified. Future work may be performed by developing the proposed idea in other transform domains such as contourlets and also extending the ML detection to correlated coefficients. Besides, turning the proposed method completely to a non-blind scheme, we can achieve both registration and statistical analysis.

REFERENCES

[1] I. J. Cox, J. Kilian, F. T. Leighton, and T. Shamoon, "Secure spread spectrum watermarking for multimedia," *IEEE Trans. Image Process.*, vol. 6, no. 12, pp. 1673–1687, 1997.

[2] M. Barni and F. Bartolini, *Watermarking Systems Engineering: Enabling Digital Assets Security and Other Applications,* CRC, 2004.

[3] Q. Cheng and T.S. Huang, "Robust optimum detection of transform domain multiplicative watermarks," *IEEE Trans. signal Processing*, **51**, vol. 4, pp. 906–924, 2003.

[4] J. Wang, G. Liu, Y. Dai, and J. Sun, "Locally optimum detection for Barni's multiplicative watermarking in DWT domain" , *Signal Processing*, vol. 88, pp. 117–130, 2008.

[5] Z. Wang and A.C. Bovik, "Image Quality Assessment: From Error Visibility to Structural Similarity," *IEEE Trans. Image Process.*, vol. 13, no. 4, pp. 600–612, 2004.

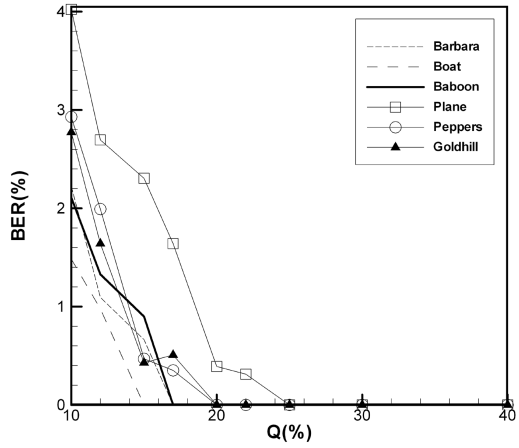

Figure 3: JPEG compression attack with various quality factors.

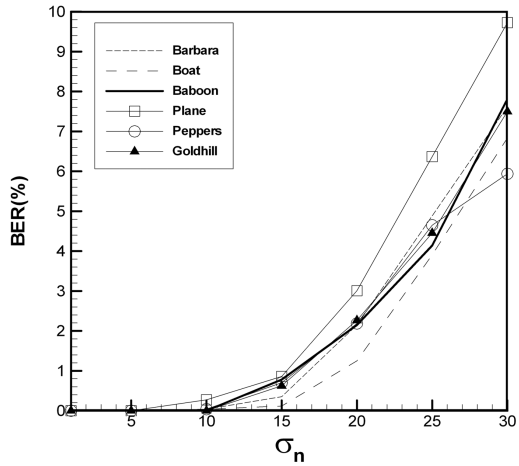

Figure 4: AWGN attack for various test images with different noise variances.

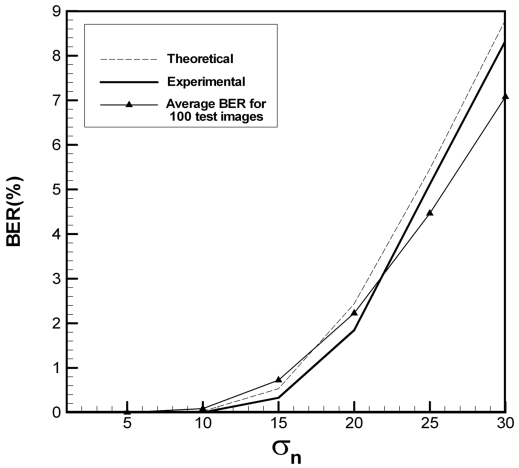

Figure 5: Comparison between the theoretical error probability, experimental result and BER averaged over 100 test images.

[6] T. M. Ng and H. K. Garg, "Maximum-Likelihood Detection in DWT Domain Image watermarking Using Laplacian Modeling," *IEEE Signal Processing Lett.*, vol. 12, no. 4, pp. 285–288, 2005.

Table 3: Comparison between our method and MWT-EMD method [11] : BER (%) under JPEG compression attack

Method	Image	PSNR	Code Length	JPEG Quality Factor	
				5	10
MWT-EMD [11]	Baboon	42 dB	64	4.69	0.00
Proposed	Baboon	42 dB	64	0.00	0.00
MWT-EMD [11]	Peppers	42 dB	64	6.25	0.00
Proposed	Peppers	42 dB	64	0.78	0.00
MWT-EMD [11]	Goldhill	42 dB	64	10.94	0.00
Proposed	Goldhill	42 dB	64	0.70	0.00

Table 4: Comparison between our method and MWT-EMD method [11] : BER (%) under AWGN attack

Method	Image	PSNR	Code Length	Noisy image PSNR(dB)			
				13	15	17	19
MWT-EMD [11]	Baboon	42dB	64	25.00	6.00	1.00	0.10
Proposed	Baboon	42dB	64	1.56	0.47	0.08	0.00
MWT-EMD [11]	Peppers	42dB	64	22.00	6.00	1.00	0.10
Proposed	Peppers	42dB	64	3.13	1.25	0.23	0.00
MWT-EMD [11]	Goldhill	42dB	64	22.50	6.00	1.00	0.10
Proposed	Goldhill	42dB	64	1.88	0.16	0.20	0.00

Table 5: Comparison between our method and MWT-EMD method [11] : BER (%) under Median Filtering attack

Method	Image	PSNR	Code Length	Median Filter		
				5×5	7×7	9×9
MWT-EMD [11]	Baboon	42 dB	64	12.50	12.50	78.13
Proposed	Baboon	42 dB	64	1.72	4.77	9.53
MWT-EMD [11]	Peppers	42 dB	64	7.81	9.36	51.56
Proposed	Peppers	42 dB	64	0.00	0.00	3.20
MWT-EMD [11]	Goldhill	42 dB	64	9.38	9.38	69.69
Proposed	Goldhill	42 dB	64	0.70	1.56	5.62

Table 6: Comparison between our method and WTGM method [12] : BER (%) under JPEG compression, and Median Filtering attacks

Method	Image	PSNR	Code Length	JPEG $Q=30\%$	JPEG $Q=50\%$	Median 4×4
WTGM [12]	Pepp	39.8 dB	512	8.40	3.10	22.05
Proposed	Pepp	39.8 dB	512	0.00	0.00	15.58
WTGM [12]	Gold	38.7 dB	512	2.35	0.20	17.60
Proposed	Gold	38.7 dB	512	0.00	0.00	5.18

[7] A. B. Watson, J.Y. Yang, J.A., Solomon, and J. Villasenor, "Visibility of wavelet quantization noise," *IEEE Trans. Image Process.*, vol. 6, no. 8, pp. 1164–1175, 1997.

[8] M. K. Mihcak, I. Kozintsev, K. Ramchandran, and P. Moulin, "Low-complexity image modeling based on statistical modeling of wavelet coefficients," *IEEE Signal Process. Lett.*, vol. 6, no. 12, pp. 300–303, 1996.

[9] D.L. Donoho and I. M. Johnstone, "Ideal spatial adaptation via wavelet shrinkage," *Biometrika*, vol. 81, pp. 425-455, 1994.

[10] F. Gembicki and Y. Haimes, "Approach to performance and sensitivity multiobjective optimization: The goal attainment method", *IEEE Transactions on Automatic Control*, **20**, vol. 6, pp. 769–771, 1975.

[11] N. Bi, Q. Sun, D. Huang, Z. Yang, and J. Huang, "Robust Image Watermarking Based on Multiband Wavelets and Empirical Mode Decomposition," *IEEE Trans. Image Processing*, vol. 16, no. 8, pp. 1956–19966, 2007.

[12] M.J. Tsai, and C.H. Shen, "Wavelet Tree Group Modulation (WTGM) for Digital Image Watermarking, " in *Proc. ICASSP*, 2007, vol. 2, pp. 173–176.